



# Office 3D-printing in paediatric orthopaedics: the orthopaedic surgeon's guide

Kai Yet Lam<sup>1^</sup>, Chui Wai Mun Mark<sup>2</sup>, Sze Ying Yee<sup>3</sup>

<sup>1</sup>KK Women's and Children's Hospital, Singapore, Singapore; <sup>2</sup>KK Women's and Children's Hospital, Singapore, Singapore; <sup>3</sup>Singapore General Hospital, Singapore, Singapore

*Contributions:* (I) Conception and design: KY Lam; (II) Administrative support: CWM Mark, SY Yee; (III) Provision of study materials or patients: KY Lam; (IV) Collection and assembly of data: All authors; (V) Data analysis and interpretation: All authors; (VI) Manuscript writing: All authors; (VII) Final approval of manuscript: All authors.

*Correspondence to:* Lam Kai Yet. Department of Orthopaedic Surgery, 100 Bukit Timah Road Singapore 229899, Singapore. Email: kaiyet@yahoo.com.

**Background:** 3D-printing, or additive manufacturing has become increasingly popular across scientific and engineering fields. The same trend has been observed in the medical field, with the main users being the dentists and the neurosurgeons. Within orthopaedic surgery, usage has been limited by accessibility and costs. The benefits of a 3D printed model in surgical planning and education in orthopaedic surgery is obvious, especially in fields like deformity correction and fracture fixation.

**Methods:** An in-house 3D-printing facility was set up, with workflow processes defined. We utilised the described workflow to 3D-print models for four paediatric orthopaedic patients with differing pathologies.

**Results:** These case examples show how 3D-printing of surgical models was easily performed, and they are useful in various clinical scenarios within paediatric orthopaedics. The steps involved in the process are accurately detailed, and are reproducible by any orthopaedic surgeon. The benefits of the application of 3D models in the deformity assessment and surgical planning of these cases are discussed individually.

**Conclusions:** An in-house 3D-printing facility is useful in paediatric orthopaedics due to the variety of complex pathologies and anatomy. We have shown that it is easy to set up with a defined work process. We advocate the application of this emerging technology into every orthopaedic practice.

**Keywords:** 3D-printing; paediatric orthopaedics

Submitted Aug 11, 2020. Accepted for publication Dec 31, 2020.

doi: 10.21037/tp-20-236

View this article at: <http://dx.doi.org/10.21037/tp-20-236>

## Introduction

3 dimensional (3D)-printing, also known as additive manufacturing, or rapid prototyping has become increasingly popular across scientific and engineering fields. The same trend has been observed in the medical field, with the main users being dentists, oro-maxillofacial and neurosurgeons (1). Within orthopaedic surgery, a literature search review in 2018 showed that there were only 237 articles on PubMed, and 269 on SCOPUS (2). The authors also concluded that, 'Presently, 3D printing is in a primitive stage in the field of orthopaedic surgery as our knowledge is

still insufficient, and costs and learning curve are somewhat high.' Through this paper, our team aims to show that the use of 3D-printing in our clinical practice is useful, easily accessible, need not be costly, and has a gentle learning curve once certain instructions are set in place. We present case examples of how 3D-printing of surgical models was easily performed by our team, and how we utilised the models in the various clinical scenarios within paediatric orthopaedics. The steps involved in the process are accurately detailed, and are reproducible by any orthopaedic surgeon.

<sup>^</sup> ORCID: 0000-0002-4058-9038.

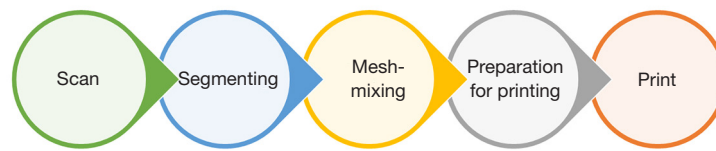


**Figure 1** Workflow for office 3D-printing.

We present the following article/case in accordance with the MDAR checklist (available at <http://dx.doi.org/10.21037/tp-20-236>).

## Methods

The entire 3D printing process can be summarised in *Figure 1*.

### Scan

Scans of the patient are usually obtained via one of the following means: Computed tomography (CT), Magnetic resonance imaging (MRI), ultrasound or surface scanners. For bone morphology, CT scan creates the easiest files to work with. MRI and ultrasound images are more tedious to segment. If fine details are important (e.g., intra-articular fractures) it is important to ask for fine-cuts (<0.5 mm) to be uploaded for better resolution during the subsequent data conversion. The quality of the final 3D print is decided by the quality of the scan images.

### Segmenting

Scans are usually saved in the Digital Imaging and COMmunications (DICOM) format (3). These need to be extracted into a 3D graphic file. Although they have more efficient features, commercially available segmenting software (e.g., Materialise MIMICS, Belgium) are expensive. Our team has found free-for-download segmenting software to be available and equally effective for the purpose of 3D modelling. These include 3D Slicer (v4.10.2. <https://www.slicer.org>. Copyright 2019 Brigham and Women's Hospital and 3D Slicer contributors), Invesalius (Developed at CTI (Renato Archer Information Technology Center) or Osirix (Proprietary license GNU LGPL since 2010). All our segmenting was performed using the software, 3D Slicer. To create bone models, we are able to do so rapidly using the following steps.

- ❖ Select “Surface Models”, then select “Grayscale Model Maker”
- ❖ Choose “Input Volume”
- ❖ Select “Create New Model” in Output Geometry
- ❖ Choose a threshold value between 200 to 240 and smoothing between 10 to 18, then click “Apply”
- ❖ The generated 3D reconstruction image can then be saved into a 3D file format (.stl or .3mf or .obj).

An example of the segmenting process is shown in *Figure 2*.

### Mesh-mixing

Mesh-mixing refers to any final edits on the reconstructed 3D file. We found the freeware Meshmixer (from Autodesk, California, United States) to be the most useful for this purpose. Unwanted segments from the 3D file can be easily deleted. Features on the 3D file can either be emphasised or masked. Erroneous print areas can be corrected via the “Analysis” and then “Repair” tabs.

### Preparation for printing

This step converts the edited and repaired 3D file into a printable version recognized by the 3D-printer. Each printer usually has its' own preferred programme. All our prints are done using the Cura program (Cura version 4.0, LPGLv3, Ultimaker. Website: <https://ultimaker.com/software/ultimaker-cura>). The files are then saved into a g-code and transferred to the 3D printer.

### Print

3D printer: There are numerous types of 3D printers available. For purpose of 3D modelling in orthopaedics, a Finite-Definition-Modeling (FDM) printer is our choice due to its low cost, and capability to print in several types of plastics (4). The Ultimaker 3 Extended 3D FDM printer (Geldermalsen, Netherlands) is currently available for USD

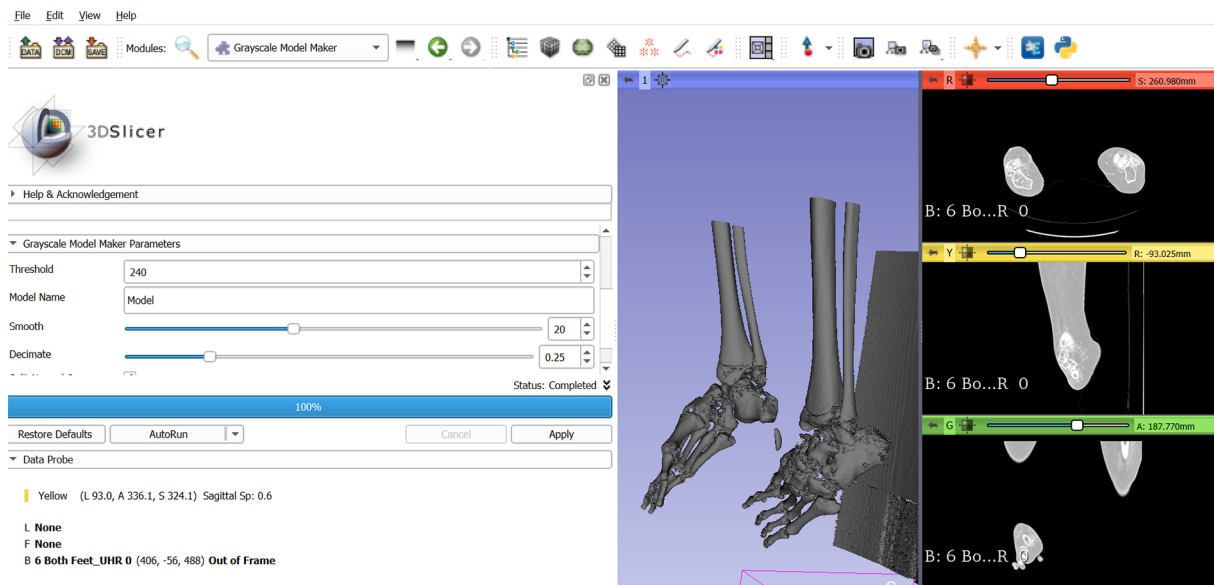


**Figure 2** Segmenting process using 3DSlicer. A threshold of 240 has been chosen using Grayscale Model Maker to allow segmentation of the bony components of the CT scan.

\$5,000.

**Print Material:** FDM printers are capable of printing in several materials. All our prints are performed using polylactic acid (PLA) material, which is capable of simulating cortical and cancellous bone. A 1 kg roll of PLA filament (2.85 mm) is available from Ultimaker at USD \$50. Most 3D models are able to be printed using about 50 to 500 g of PLA filament.

Most printers have their preferred settings in terms of print temperature, print speed and retraction speed. We recommend the following settings for optimal print:

- ❖ Quality: 0.15 mm (usually under normal settings);
- ❖ Layering Height: 2 mm;
- ❖ Supports: Yes;
- ❖ Infill: 10% to 20%, gyroid.

### Statistical analysis

There was no statistical analysis required for this article.

### Ethical statement

The trial was conducted in accordance with the Declaration of Helsinki (as revised in 2013). This study has been approved by the Singhealth Centralised Institutional Review Board CIRB Ref: 2020/2592 and informed consent has been obtained from the participants.

## Results

We have successfully utilized the above workflow to create 3D models that have helped us in the pre-operative deformity assessment and surgical simulation of several patients. A discussion on each individual case is presented below.

### Case 1: Correction of rigid cavovarus deformity

The patient is a 13-year-old boy with background history of spina bifida and bilateral rigid cavovarus foot deformities. He had undergone several surgical procedures before, but has significant residual deformities bilaterally. Due to the severity and rigidity of the deformity, we planned to use gradual correction using a Taylor Spatial Frame (TSF), Smith and Nephew, USA. The 3D model allowed us to accurately assess the severity of the deformities in the midfoot and hindfoot. He was noted to have a varus angulation of 60 degrees, apex dorsal sagittal deformity of 50 degrees, and supination of 45 degrees in the midfoot. The hindfoot equinus and varus deformity was assessed to be minimal, and unnecessary to be addressed with the frame. We believe that the amount of midfoot supination is better assessed with the help of the 3D model. 3D reconstructions of the CT scans are unable to assess the supination accurately, as they are viewed through a 2D

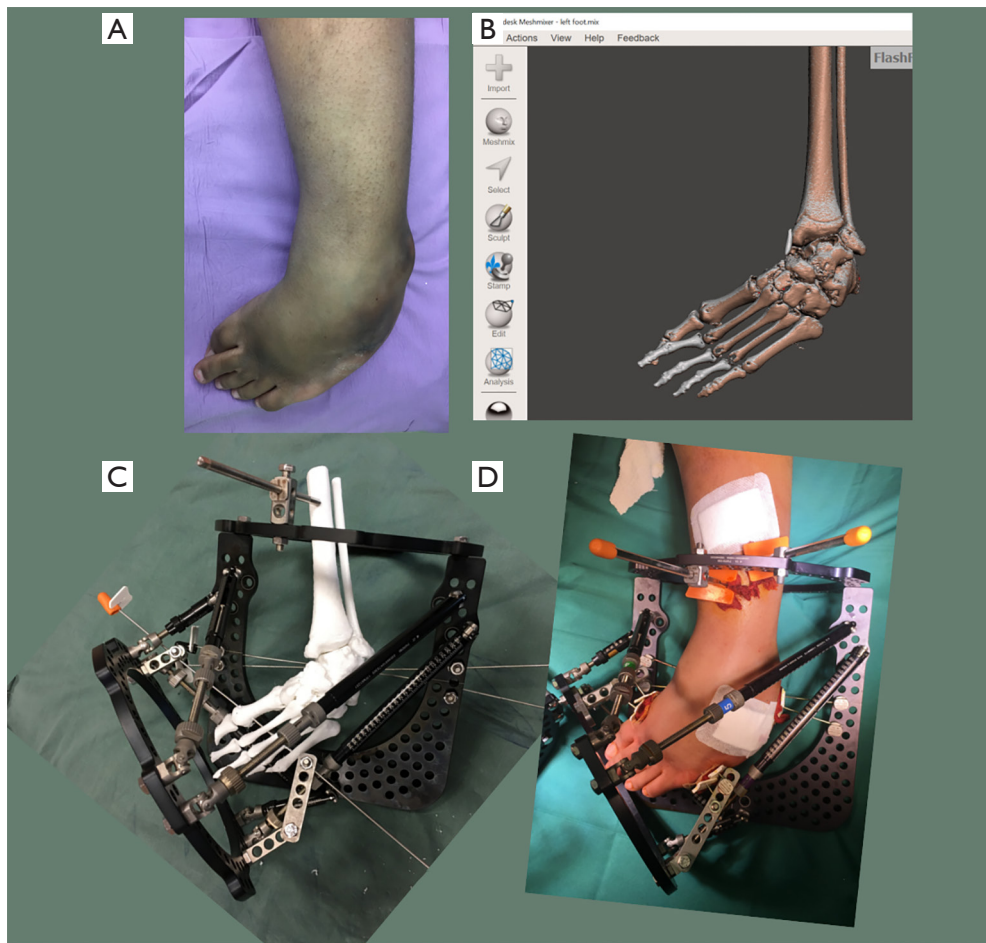


**Figure 3** This shows how the process of 3D modelling of a severely deformed foot, and translating pre-surgical simulation into actual surgery. (A) Pre-operative photograph of the left foot showing severe forefoot and midfoot deformities. (B) MeshMixing allows editing of the reconstructed 3D file, allowing repairs of the model surfaces before printing. (C) Pre-surgical simulation allows identification of any intra-operative difficulties. (D) Reproducing the pre-surgical plan intra-operatively.

monitor screen. There are various TSF frame constructs that are suited for different deformity parameters. Based on our patient's deformity assessment, we decided on the butt frame construct.

The 3D model also allowed us to simulate the corrections through midfoot or hindfoot osteotomies. They also allowed a visual appreciation of the final correction using the deformity parameters, and the chosen butt frame construct. In addition, we were able to anticipate intra-operative difficulties such as the foot being too short, and the frames abutting each other. These problems were easily overcome by choosing a 2/3 forefoot ring, and proper pre-operative planning of our ring positions and wire attachment supports. Post-operatively, we could also

assess the mounting parameters of the reference ring more accurately than using standard X-rays with the help of the 3D model.

The patient achieved successful correction of his bilateral feet deformities without any need for any unplanned revisions of the frame during the correction and consolidation phases.

- ❖ Weight of print: 137 g;
- ❖ Estimated cost: USD \$6.85;
- ❖ Print Time: 23 hours and 0 minutes.

See *Figure 3* for the pre-operative and intra-operative photographs. *Figure 4* shows a successful correction using the same deformity parameters that were assessed using the 3D model.



**Figure 4** Post-operative photographs of the patient's left foot showing excellent correction of the deformity and lengthening of the foot.

### *Case 2: Comminuted calcaneus fracture*

This patient is an 11-year-old boy who suffered a fall from height, with several injuries including a subdural hematoma, rib fractures with hemopneumothorax and a comminuted right calcaneal fracture. X-rays and CT scans confirmed a joint-depressed, Sanders (5) type III calcaneal fracture.

3D-modelling allowed us to appreciate the anatomy of the comminuted fragments, and understand how to achieve a reduction using an Ollier's approach, which is a much smaller exposure than the traditional lateral L-flap approach. This approach is usually more appropriate for simpler fracture patterns, but we were able to achieve near anatomical reduction of the fracture fragments with the aid of the 3D model. The 3D model allowed us to perform a pre-surgery simulation of the reduction procedure, using a Schanz pin to elevate the depressed posterior facet, followed by reduction of the anterior and middle facets under direct vision. An appropriately sized calcaneal plate was chosen pre-operatively based on the best fit obtained with the 3D-model (Paragon 28 Medium Calcaneal plate, USA).

The patient recovered well post-operatively and was able to ambulate with full weight-bearing on the right foot 4 months after surgery.

- ❖ Weight of print: 154 g;
- ❖ Estimated cost: USD \$7.70;
- ❖ Print Time: 25 hours and 11 minutes.

Figure 5 shows the radiographs, CT scans, pre-surgical simulation and the post-operative radiographs and clinical photograph.

### *Case 3: Arthroscopy-assisted percutaneous screw fixation of a triplane ankle fracture*

Our patient is a 13-year-old boy who sustained a right ankle triplane fracture. X-rays showed displacement necessitating manipulation and reduction (see Figure 6), and CT scan confirmed a 2-part triplane fracture.

The 3D-model allowed us to appreciate the complex anatomy of the triplanar fracture. While this may be intuitive to most experienced paediatric orthopaedic surgeons, it may not be so for the general orthopaedist. Having the 3D-model in hand allowed us to plan and simulate a percutaneous screw fixation of the fracture, with the position of the reduction clamp and trajectory of the guidewire and percutaneous screws decided pre-operatively. The procedure was carried out as planned and an ankle arthroscopy was then performed to confirm the adequacy of the articular reduction. See Figures 7 and 8.

Surgically simulating the position of the reduction clamp and trajectory of the percutaneous screws allowed us to have maximal compression perpendicular to the fracture plane. The percutaneous procedure also allowed small incisions that facilitated faster wound healing and rehabilitation.

- ❖ Weight of print: 202 g;
- ❖ Estimated cost: USD \$10.10;
- ❖ Print Time: 31 hours and 28 minutes.

### *Case 4: Correction of adolescent Blount's disease*

The patient is a 15-year-old boy with the diagnosis of right adolescent Blount's disease. He presented with a right genu varus deformity, and had undergone lateral proximal

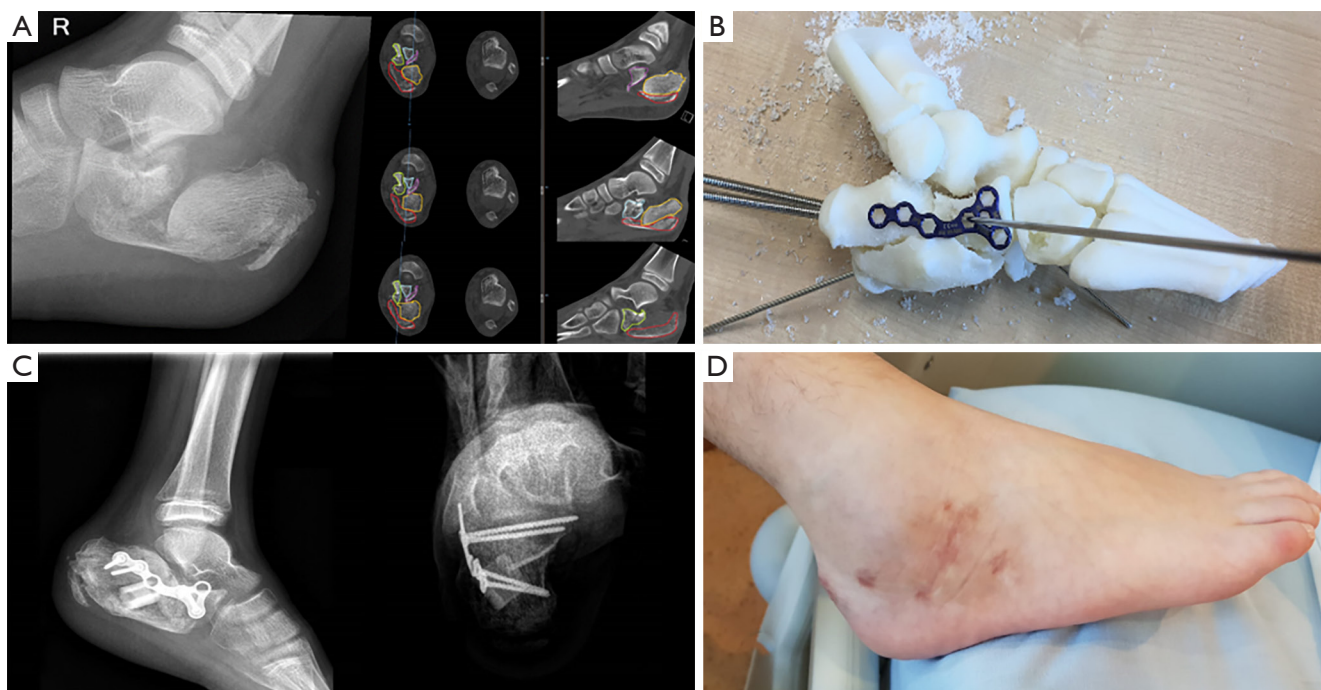


**Figure 5** The use of 3D-modelling in selecting the implant, and positioning of the implant for a calcaneal fracture. (A) Pre-operative lateral radiograph and CT scan of the right foot. (B) Surgical simulation using a 3D-printed model. Schanz screws have been placed through the calcaneus to elevate the posterior tubercle, and an appropriately-sized implant is chosen. There was no need for any pre-contouring of the implant. (C) Post-operative radiographs using the implant selected. (D) Clinical photograph showing good wound healing with a smaller incision.



**Figure 6** Pre-operative radiographs of the right ankle triplane fracture. A manipulation and reduction was performed in the emergency department before a CT scan was ordered. (A) Anteroposterior view; (B) lateral view.

tibia hemiepiphyseodesis previously, with no significant correction.

Deformity assessment with the 3D-printed model showed a proximal tibia varus deformity of 24 degrees, procurvatum of 22 degrees, and internal rotation of 20 degrees. Assessment of the degree of tibia rotation was difficult using the X-rays, CT scan and clinical findings. However, this was easily performed using the 3D model, and a surgical simulation allowed us to view the post-correction foot and ankle position, based on a deformity parameter of 20 degrees of internal rotation. We accounted for 7 degrees of varus deformity from the distal femur by over-correcting the End-of-correction parameters, and also added 12 mm of lengthening at the osteotomy site.

Pre-surgical simulation allowed us to plan the appropriate osteotomy site, mounting position of the reference ring, and visually appreciate the post-correction limb alignment using the planned deformity parameters. For large degrees of deformity correction, especially when there is significant rotation correction of 20 degrees

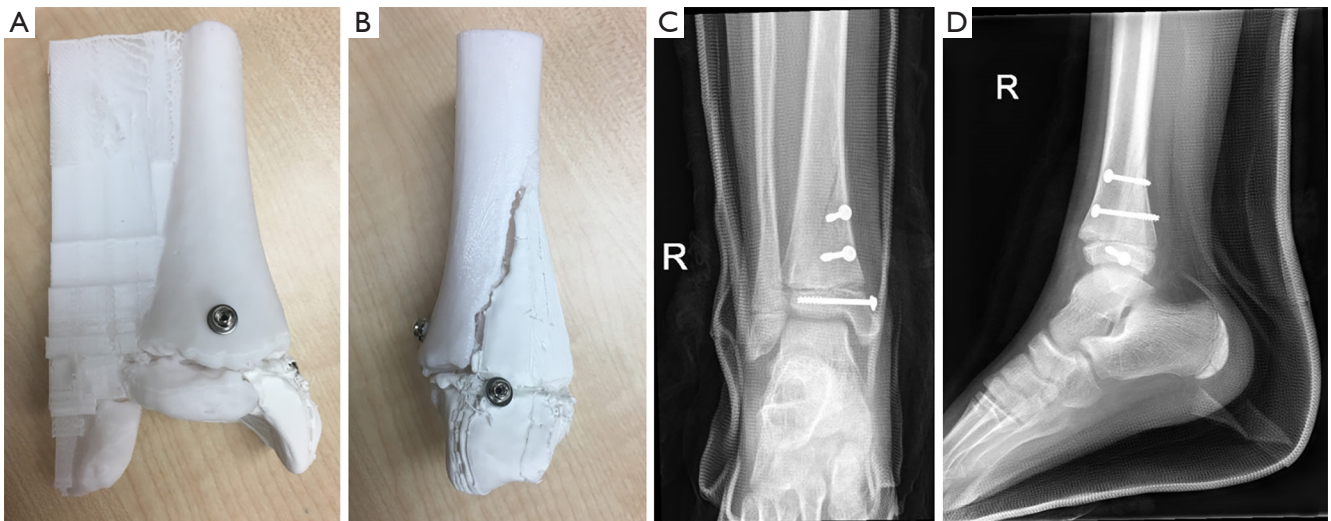


**Figure 7** Figure shows the pre-surgical simulation of fracture fixation of a paediatric triplane ankle fracture, and the translation of the plan into actual surgery. (A and B) Surgical simulation on a 3D printed model allows 3-dimensional appreciation of the fracture pattern, and best trajectory of the screw to obtain good fracture compression. The print supports holding the tibia and fibula together have not been removed. These supports are often left intact if they do not interfere with the surgical simulation. (C and D) Immediate post-operative radiographs.



**Figure 8** The use of 3D modelling has allowed us to plan for the surgery using smaller wounds. (A) Clinical photograph showing small wounds for percutaneous screw fixation and arthroscopic confirmation of reduction. (B and C) Intra-operative ankle arthroscopy images showing perfect reduction of the articular surface.

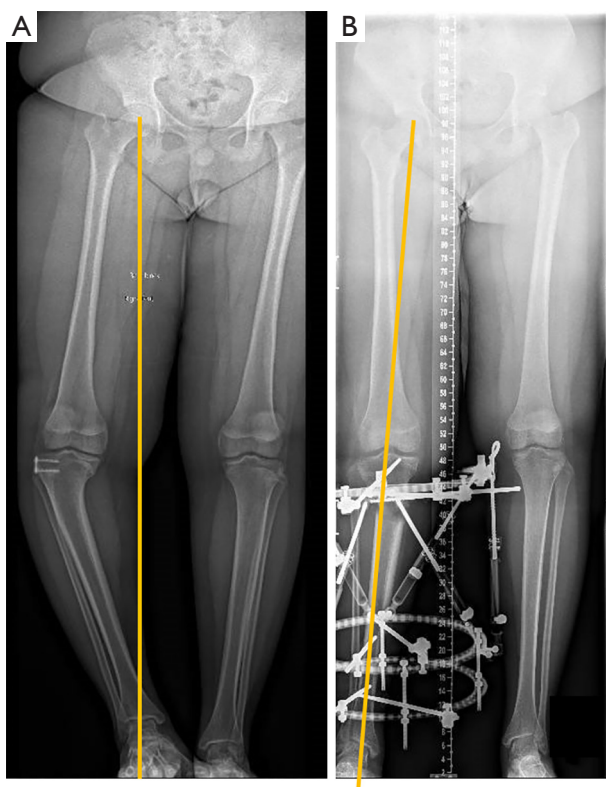


**Figure 9** Pre- (A) and post- (B) correction radiographs of Case 4, showing good correction of the mechanical axis.

or more, we find that a pre-surgical simulation using 3D-printed models allows us to run the program physically, and anticipate any overlapping or obstructing struts during the correction phase.

Figure 9 shows the pre- and post-correction radiographs of the patient. Figure 10 shows the full-length 3D-printed tibia model and pre-surgical simulation, as well as the pre- and post-correction clinical photographs.

The deformity was corrected using deformity parameters determined using the 3D-printed model, and there was no need for any change in the correction program or any unplanned change of the struts or pin sites during the correction phase.

- ❖ Weight of print: 460 g;
- ❖ Estimated cost: USD \$23.00;
- ❖ Print Time: 65 hours, 41 minutes.

### Conclusions

A review of the existing literature regarding 3D printing in paediatric orthopaedic surgery, shows some case series and case reports. Otsuki *et al.* (6), Zheng *et al.* (7) and Zhou *et al.* (8) have all utilised 3D printing to create navigation templates and cutting guides for the purpose of corrective surgeries in paediatric hip disease and periacetabular

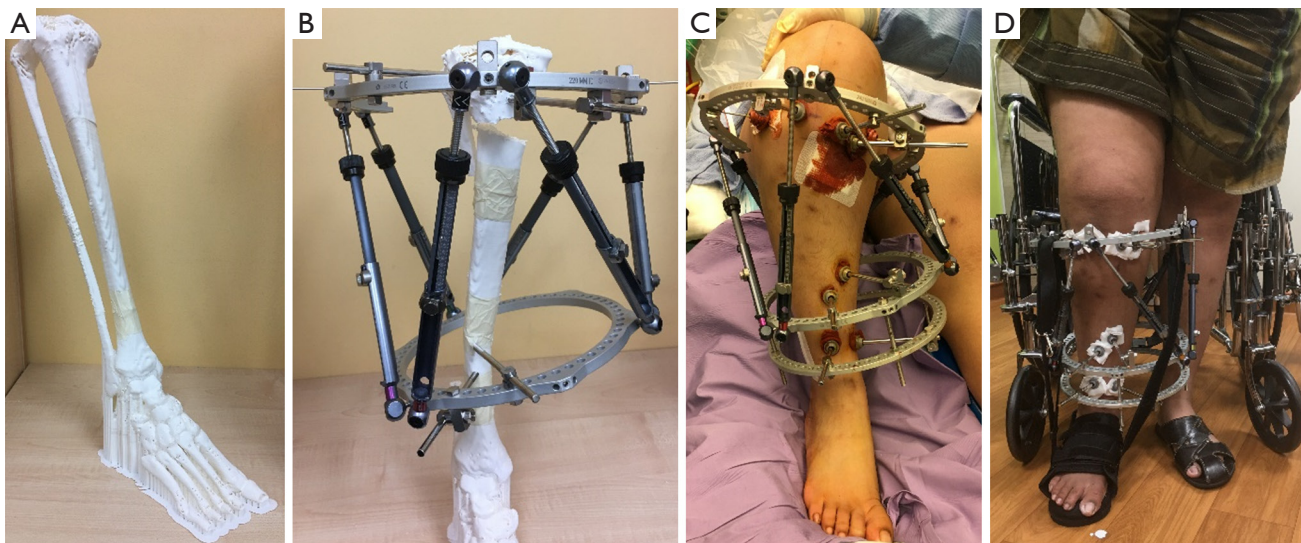


**Figure 10** Pre-surgical simulation on a full-length 3D-printed model leading to a successful clinical outcome.





**Figure 11** An example of a 3D print with an infill of 20% with gyroid structure, resembling the tactile feel of cancellous bone.

osteotomies. Surgery with these navigation templates have shown reduced intraoperative damage to the femoral neck epiphysis, decrease operation time, reduce intraoperative hemorrhage, and decrease radiation exposure. Burzyńska *et al.* (9) also documented a case report of the use of 3D modelling in the pre-surgery planning of an Ilizarov frame application for limb lengthening and axial correction in a 3-year-old patient.

We have found in our clinical practice that office 3D-printing is useful in paediatric orthopaedic surgery for deformity and fracture assessment, pre-surgical simulation, patient and resident education.

There are certain limitations to our 3D-modelling technique discussed here. The size of any single 3D print is limited by the dimensions of the 3D-printer. This is termed the maximum build size. For our chosen 3D-printer, the maximum build size is 215 mm × 215 mm × 300 mm. For larger models like Case 4 where the entire tibia or lower limb is to be reproduced, the print has to be divided into several segments. Attachment pegs and corresponding peg-holes are inserted manually into the segmented 3D file using the MeshMixer programme for easy re-attachment after printing. In addition, while cortical bone is accurately reproduced using the above technique, cancellous bone is not. Drilling and screwing into the bone models may

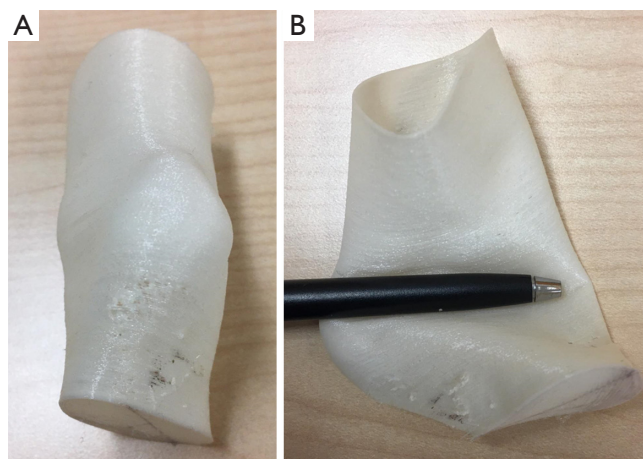


**Figure 12** Experiment in using TPU to print the skin envelope. (A) 3D-printed model of the skin envelope of a left knee. The patella and condylar bone prominences are easily appreciated. (B) The model is easily compressible, but maintains elastic properties, making it suitable for manipulation during pre-surgical simulation.

not give the practising surgeon the same tactile feel that they would expect intra-operatively. We have found that using an infill of 20% with a gyroid structure can give some semblance of cancellous bone during the pre-operative surgical simulation (see *Figure 11*). The size of the soft tissue has also an important role to play during the pre-surgical planning for hexapod and Ilizarov frames. We have experimented with the use of flexible printing materials like thermoplastic polyurethane (TPU) to 3D print the soft tissue envelope (see *Figure 12*). Our results are not ready for publishing at present, but it does seem quite feasible to incorporate into future 3D models that require reproduction of the soft tissue envelopes for surgical planning.

To our knowledge, there has been no documented use of 3D-modelling in pre-surgical simulation and planning for pediatric calcaneal fractures, Taylor spatial frame application for cavovarus foot deformity, Blount's disease and arthroscopy-assisted percutaneous screw fixation of an ankle triplane fracture. Previous publications on the use of 3D-modelling also do not have details about their segmenting or printing techniques.

This paper serves to document the usefulness of the office 3D-printer, and how creating an anatomical model can be easy, reproducible, and cost-efficient. The benefits

of having this facility within the hospital or department include the following:

- (I) Customisation of anatomical models for surgical planning, which includes best surgical approach and use of implants. This can be potentially advantageous in reducing surgical time and implant wastage. Pre-surgical simulation of the Taylor Spatial frames and pre-contouring of fixation plates have been found to be useful in reducing surgical time, as well as ensuring that all necessary implants are available ahead of time. Duplicates of models are also useful in medical education, allowing surgical trainee to have hands-on experience, devising surgical methods appropriate for a surgical case.
- (II) Increased cost efficiency. The cost of 3D printing for small production runs, and simple anatomical models, can be much lower than that of commercialised 3D production. Models can also be conveniently printed within hours as compared to that in the printing companies which may take days or even weeks.
- (III) Protection of patient confidentiality. The availability of 3D printing facility within the hospital means that all patient data can be handled safely within the hospital, without risks of exposing confidential information (i.e., patient identifiers, diagnoses) to printing companies.

## Acknowledgments

*Funding:* This work was supported by SingHealth Duke NUS Musculoskeletal ACP research grant. (Grant Number: 13/FY2018/P2/08-A51).

## Footnote

*Reporting Checklist:* The authors have completed the MDAR checklist. Available at <http://dx.doi.org/10.21037/tp-20-236>

*Data Sharing Statement:* Available at <http://dx.doi.org/10.21037/tp-20-236>

*Conflicts of Interest:* All authors have completed the ICMJE uniform disclosure form (available at <http://dx.doi.org/10.21037/tp-20-236>). The authors have no conflicts of interest to declare.

*Ethical Statement:* The authors are accountable for all aspects of the work in ensuring that questions related to the accuracy or integrity of any part of the work are appropriately investigated and resolved. The trial was conducted in accordance with the Declaration of Helsinki (as revised in 2013). The study was approved by institutional/regional/national ethics/committee/ethics board of SingHealth Centralized Institutional Review Board (CIRB Ref: 2020/2592) and informed consent was taken from all the patients.

*Open Access Statement:* This is an Open Access article distributed in accordance with the Creative Commons Attribution-NonCommercial-NoDerivs 4.0 International License (CC BY-NC-ND 4.0), which permits the non-commercial replication and distribution of the article with the strict proviso that no changes or edits are made and the original work is properly cited (including links to both the formal publication through the relevant DOI and the license). See: <https://creativecommons.org/licenses/by-nc-nd/4.0/>.

## References

1. Hoang D, Perrault D, Stevanovic M, et al. Surgical applications of three-dimensional printing: a review of the current literature & how to get started. *Ann Transl Med* 2016;4:456.
2. Vaishya R, Patralekh MK, Vaish A, et al. Publication trends and knowledge mapping in 3D printing in orthopaedics. *J Clin Orthop Trauma* 2018;9:194-201.
3. Graham RN, Perriss RW, Scarsbrook AF. DICOM demystified: a review of digital file formats and their use in radiological practice. *Clin Radiol* 2005;60:1133-40.
4. Mertz L. Dream it, design it, print it in 3-D: what can 3-D printing do for you? *IEEE Pulse* 2013;4:15-21.
5. Sanders R, Fortin P, DiPasquale T, et al. Operative treatment in 120 displaced intraarticular calcaneal fractures. Results using a prognostic computed tomography scan classification. *Clin Orthop Relat Res* 1993;290:87-95.
6. Otsuki B, Takemoto M, Kawanabe K, et al. Developing a novel custom cutting guide for curved peri-acetabular osteotomy. *Int Orthop* 2013;37:1033-8.
7. Zheng P, Yao Q, Xu P, et al. Application of computer-aided design and 3D-printed navigation template in Locking Compression Pediatric Hip Plate™ placement for pediatric hip disease. *Int J Comput Assist Radiol Surg* 2017;12:865-71.
8. Zhou Y, Kang X, Li C, et al. Application of a 3-dimensional

printed navigation template in Bernese periacetabular osteotomies. A cadaveric study. *Medicine (Baltimore)* 2016;95:e5557.

9. Burzyńska K, Morasiewicz P, Filipiak J. The Use of 3D Printing Technology in the Ilizarov Method Treatment: Pilot Study. *Adv Clin Exp Med* 2016;25:1157-63.

**Cite this article as:** Lam KY, Mark CWM, Yee SY. Office 3D-printing in paediatric orthopaedics: the orthopaedic surgeon's guide. *Transl Pediatr* 2021;10(3):474-484. doi: 10.21037/tp-20-236